UCRL-ID-131907

Advanced Composites Technology

S. J. DeTeresa, S. E. Groves, and R. J. Sanchez

October 1998

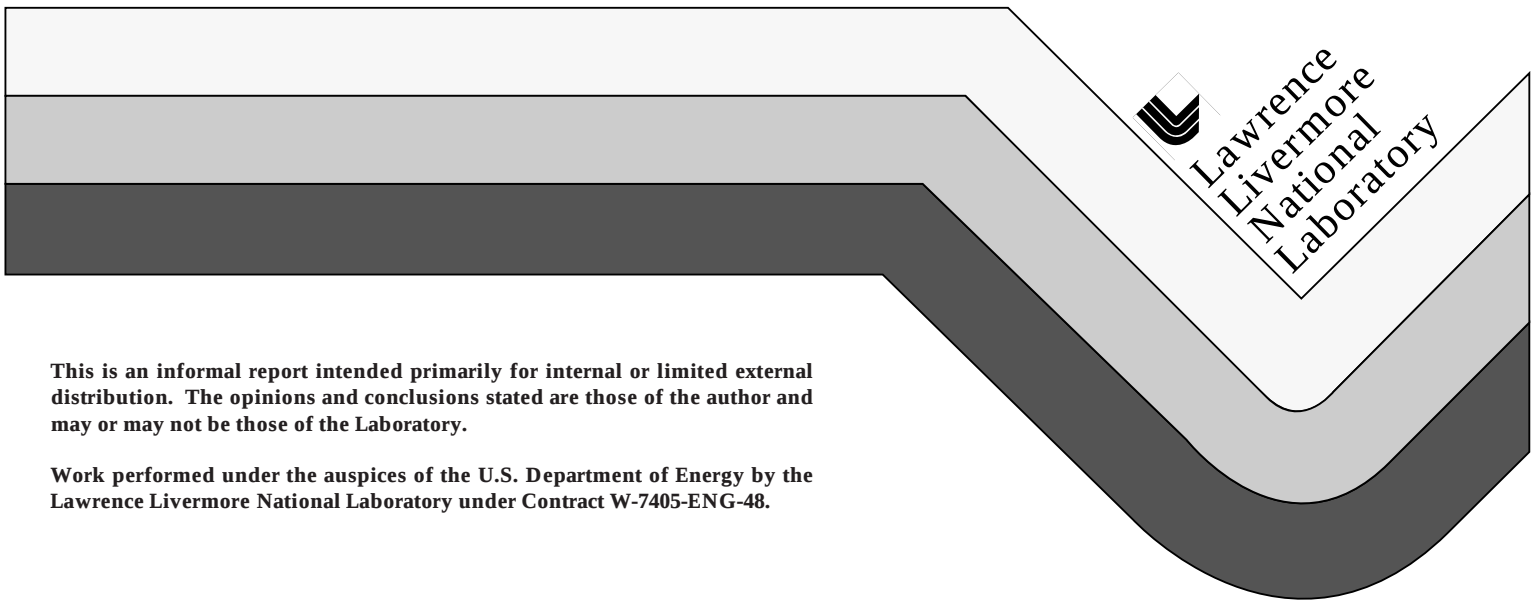

Work performed under the auspices of the U.S. Department of Energy by the Lawrence Livermore National Laboratory under Contract W-7405-ENG-48.

Advanced Composites Technology

S. J. DeTeresa, S. E. Groves, and R. J. Sanchez
Lawrence Livermore National Laboratory
(925) 422-6466
deteresa@llnl.gov

Abstract

The development of fiber composite components in next-generation munitions, such as sabots for kinetic energy penetrators and lightweight cases for advanced artillery projectiles, relies on design trade-off studies using validated computer code simulations. We are developing capabilities to determine the failure of advanced fiber composites under multiaxial stresses to critically evaluate three-dimensional failure models and develop new ones if necessary. The effects of superimposed hydrostatic pressure on failure of composites are being investigated using a high-pressure testing system that incorporates several unique features. Several improvements were made to the system this year, and we report on the first tests of both isotropic and fiber composite materials. The preliminary results indicate that pressure has little effect on longitudinal compression strength of unidirectional composites, but issues with obtaining reliable failures in these materials still remain to be resolved. The transverse compression strength was found to be significantly enhanced by pressure, and the trends observed for this property and the longitudinal strength are in agreement with recent models for failure of fiber composites.

Introduction

We are studying the mechanics of failure in thick-section composites for application to sabots for long-rod, kinetic energy penetrators, advanced artillery projectiles, lightweight gun barrels for ship defense systems, and flywheel rotors as power sources for electromagnetic guns. A common need in all these applications is a proven, three-dimensional failure model for laminated orthotropic materials that is suitable for implementation into continuum computer codes. We are developing unique experimental capabilities and failure models to address these needs.

The next-generation composite sabot for the 120-mm, long-rod penetrator is currently being developed by the U. S. Army. This M829 E3 version is expected to provide significant velocity gains through several design upgrades, which include weight reduction in the composite sabot. The ability to design by analysis requires validated composite material failure models for the complex dynamic stresses generated during launch. By comparing test firing results to ply-level composite analysis, it has been established that a key to surviving launch loads is the enhancement of shear and compression strength under triaxial compression stresses. Without such a strengthening mechanism, the sabot would be expected

to fail at half the launch pressures that it has seen in numerous firings. A recent survey of the available studies on the effects of triaxial compression stresses on compression and shear strengths shows that results vary significantly.[1] The disparities are most certainly due to variations in materials, test specimens, and test methods used in the different studies. Many of the tests utilized nontraditional methods to perform tests in high-pressure cells designed for studying isotropic materials. While strength changes due to superimposed high pressure have been measured, it is clear in many of these studies that the failure modes were quite different from pure compression or shear.

In order to make the next leap in improving sabot performance, we need to have a predictive capability using existing computer simulations. The proposed design concepts incorporate new fiber architectures, structural shapes, and materials. To study the numerous combinations of these new approaches in a purely empirical manner would be impractical. We are developing a scientific approach to these issues by conducting the critical experiments to validate or develop a proven failure model. For this purpose, we have designed and constructed a triaxial compression test system that utilizes standard composite test specimens. The hardware normally used for uniaxial tests has been adapted to fit within a high-pressure cell capable of maintaining constant hydrostatic pressure up to 100 ksi during uniaxial testing. During the past year we have made additional upgrades to the system and improved testing procedures to the point where high-pressure testing can be conducted in a reliable and facile manner. The features of this test system and initial results for the effect of pressure on compression strength of isotropic and fiber composite materials will be summarized.

Experimental

System Design and Upgrades

In adapting proven composite compression test methods and fixtures for use in the confined spaces of a high-pressure vessel, a limitation is the size of the specimen relative to the bore of the vessel. The hardware required to prevent erroneous failure modes such as end-brooming and longitudinal splitting takes up a significant percentage of the cross-section. Consequently, the reaction loads generated due to pressure are nearly an order of magnitude greater than the uniaxial force required to fail even the strongest composite specimens. Furthermore, due to the relatively low compressibility of the liquid pressure medium, small fluctuations in pressure occur as the servohydraulic supply pressure unit tries to maintain a constant pressure while the piston is lowered into the vessel. A 500-psi fluctuation (which is less than 1% of the higher superimposed pressures) results in over 600 lb of reaction force on an external load cell. This amounts to approximately 10% of the failure load for some specimens and therefore can potentially mask any real changes in strength due to the triaxial stress state on the specimen. Compounding this problem with measuring load externally is the added frictional force at the high-pressure seals in the piston packing. Our original design for circumventing these problems using an internal load cell was based on measuring the deflection of a hollow piston with a Bourns potentiometer. The body of the potentiometer was mounted above the piston and the pressure seal in a hollow stand-off. In this

configuration, external loads deform the standoff and register on this “internal” load cell. In fact, we found this design to be too sensitive to friction force and pressure load. Additionally, the calibrations made against a standard load cell showed that the potentiometer cell was neither linear nor sufficiently reproducible for our purposes.

A new internal load cell was designed to fit in the existing space of the hardened Vascomax 350 CVM piston. It uses foil strain gages to measure the deflection of a column fixed at its ends to the inside of the piston. A schematic of this design is shown in Figure 1. In order to match the elastic limit of the piston and measure loads without yielding at the highest pressures, titanium was selected for the column load cell. Both the titanium and 350 CVM are elastic up to ca. 1% strain. The load cell is fixed to the piston via threads at the top. The cell is screwed into the piston cavity to generate a slight compressive preload so that a positive reading is obtained even in the unloaded condition. The upper end of the cell is attached to a portion of the piston body, which is above the pressure seal and could be affected by friction loads. However, it was found that the response is relatively insensitive to external loads because the thinnest and therefore most highly deformable regions of both the load cell and piston are on the high-pressure side of the piston packing. For this same reason, the pressure contribution to the internal load cell deflection is significantly less than in the previous design. For the time this load cell has been in use, it has provided a very stable and reproducible response.

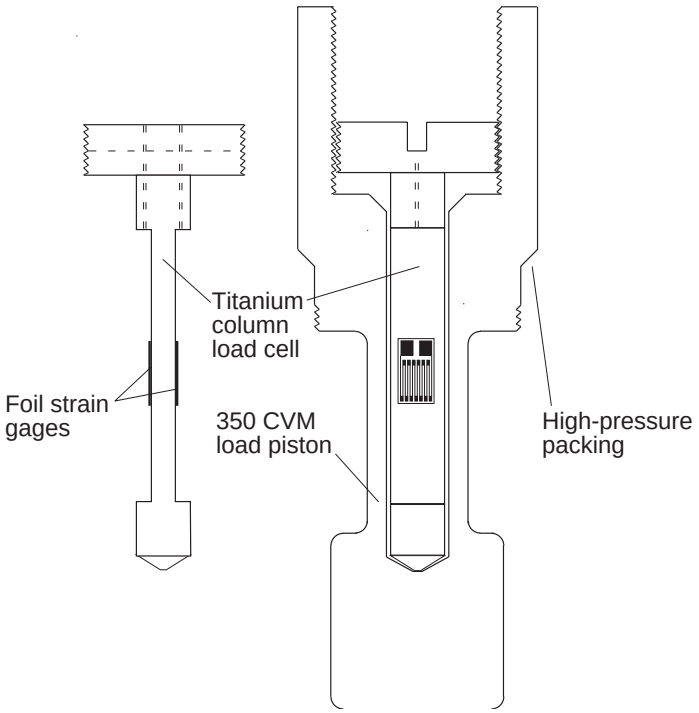

Figure 1. Titanium internal column load cell inside piston.

A Harwood strain-gaged, diaphragm pressure cell was added to the inlet line of the vessel. This pressure gage was calibrated for the range 0–100 ksi using NIST-traceable standards and is checked periodically using equivalent resistance shunts. Although manganin wire gages provide a slightly more linear response, it was decided that the strain-gaged cell was necessary for withstanding the pressure shock due to specimen unloading at failure and for allowing the use of liquids that may be incompatible with manganin. Because there is still some albeit smaller contribution of pressure to the internal load cell output, an accurate pressure reading was needed to correct this output for the pressure fluctuations mentioned earlier.

Problems were encountered early on with the use of silicone fluid for the pressure medium. Although we demonstrated last year that this fluid does not adversely affect the composite, it has the unfortunate characteristic of a large viscosity increase with pressure.[2] This viscosity build-up led to an unacceptable decrease in pressure wave speed through the small-diameter, high-pressure tubing. Other candidate liquids were considered using the following criteria: relatively low viscosity up to 100-ksi pressure, minimum hazards, sufficiently low surface tension to wet-out parts and allow air bubbles to escape freely during specimen loading, and, most importantly, no deleterious affects on the specimen properties. The liquids considered were isopropanol, ethylene glycol, and kerosene. The screening test was an immersion of composite samples under 60-ksi pressure for at least 30 minutes. This is a severe screening test since a typical high-pressure compression test requires the specimen to sit at pressure for less than 5 minutes. Weight change after exposure was used to assess the interaction between fluid and composite, and results for IM7/8551-7 are summarized in Table 1. Kerosene was found to be as inert as silicone, but ethylene glycol and especially isopropanol were taken up by the composite in appreciable quantities. Based on these results, kerosene was selected as the working fluid for all the tests reported herein.

Table 1. Effect of 30-minute exposure by IM7/8551-7 composite to three liquids at 60-ksi pressure.

	Dow 200 Silicone Fluid	Isopropanol	Ethylene Glycol	Kerosene
Avg. Wt. Change (%)	+0.010	+0.434	+0.713	+0.002
SD (%)(1)	0.009	0.004	0.019	0.004

(1) Instrumental error ≈ 0.005%

Test Specimens and Fixture

Two composite materials that have been extensively tested in sabots were investigated. A toughened epoxy matrix, 8551-7, with IM7 carbon fiber and a thermoplastic matrix, Ultem polyetherimide, with AS4 carbon fiber were obtained in unidirectional prepreg tape form. The Ultem prepreg and some molded 6-inch-square panels were supplied by Mr. Joe Morris of Fiberite, Inc. These panels were compression molded using steel tooling and exhibited the marcel defects alluded to earlier. Therefore, they were deemed unsuitable

for high-pressure testing since we have shown that the defects can degrade compression strength, but they were used to establish test conditions and procedures. We have begun to develop a process for fabricating defect-free Ultem panels using monolithic carbon tooling to match the coefficient of thermal expansion of the prepreg in the fiber direction. However, numerous attempts with compression press molding failed to produce panels having uniform thickness. The problem was traced to the deflection of the relatively soft carbon slabs under molding pressures. This problem can possibly be overcome using autoclave processing and panels will be prepared in this manner for testing in FY98.

The 8551-7 epoxy prepreg was processed by INTEC into 12-inch-square, 16-ply panels following manufacturer's recommended procedures. Ultrasonic C-scans demonstrated that all were of high quality and free of any gross porosity or delaminations.

The composite test specimen is a variant of the Boeing-modified ASTM D695 specimen. The test specimen is made of 1/2-inch-wide strips of composite with either fiberglass or carbon fiber composite tabs adhesively bonded at each end. The specimen is shown in Figure 2. It was selected because of its widespread use and compact size. The modifications to the standard specimen are those made by the group headed by Prof. F. L. Matthews at Imperial College.[3] Their work has shown that improved strengths and reduced scatter are obtained when the high shear stresses near the tab end are relieved by eliminating the adhesive bond in this area. This is done in a controlled manner by covering the gage section of the specimen with a release-coated tape that extends in the tab area, prior to bonding the tabs. We also used the slightly longer specimen examined by Matthews, which has a gage length of 0.4 inch. This allows room for mounting foil strain gages if desired.

Specimens were prepared from 6-inch by 3.5-inch composite plates that were cut using a diamond saw with flood coolant from 12-inch-square panels. The gage area was covered with 3/4-inch-wide Kapton tape with a release backing. With this width tape, the final specimens have an intentional 0.18-inch unbonded length at the tab ends. The bonding surfaces were lightly abraded then cleaned with acetone and isopropanol. Tabs 6 inches long by 1.5 inches wide were bonded to the composite using a 0.010-inch-thick film adhesive (3M AF-126-2). An aluminum alignment fixture was used during the adhesive cure to maintain the position of the tabs. The adhesive was cured in Wabash Genesis press under 50-psi pressure for one hour at 250°F. Shims were used in the alignment fixture to yield a final nominal 0.005-inch-thick adhesive bondline. After tab bonding, all four edges of the tabbed panel were trimmed with the diamond saw using a previously marked panel edge for reference. The loading edges and the surfaces of the tabs were then ground flat and parallel also under flood coolant using a surface grinder. The panel was sectioned into 0.5-inch-wide specimens using the diamond saw and then ground to 0.480-inch widths using the surface grinder. The first specimens tested were ground to a 0.499-inch width to slip fit the slot in the fixture. However, it was noted that premature failures were occurring at the fixture since this fit did not allow room for Poisson's expansion. This was especially evident for laminates having ±30 and ±45 plies since these have Poisson's ratios of 1.1 and 0.7, respectively.

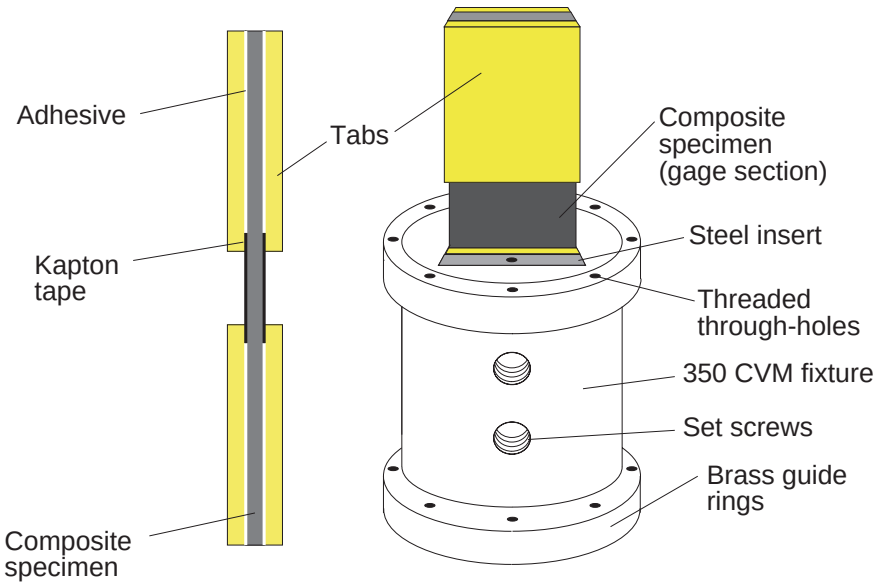

Figure 2. Compression test specimen and fixture for compression tests at high pressure.

The compression test fixture shown schematically in Figure 2 is also based on some of the work due to Matthews.[3] Two of these fixtures having precision rectangular holes were machined from 350 CVM steel. The hole is 0.500-inch wide and 0.380-inch thick. The thickness was designed to accommodate different tabbed specimens while leaving space for the steel insert, as shown in the figure. A through-thickness compression is applied to the tabs through the steel insert via two set screws on the side of the fixture. This compression has been shown to be beneficial in preventing premature tab failures in compression tests.[2] In order to prevent damage to the bore of the pressure vessel, the outer diameter of the steel fixtures is reduced and the contact with the bore is made with press-fit brass guide rings. These guide rings are machined to slip-fit the bore and thus provide precision alignment of the fixtures in the vessel.

Initial high-pressure testing with composites exposed some problems with the test fixtures. Upon failure, the stored energy in the load train is immediately released, which causes rapid compression of the liquid confined within the gage area of the specimen. The resulting pressure spike was sufficient to deform the brass guide rings and cause the top fixture to be lodged within the vessel. After several tedious extractions, this problem was solved by machining several threaded “vent” holes in all the brass rings. These holes allowed the liquid to flow past the fixture without damaging the rings, and the threads provided a method to easily extract the fixture after testing.

Compression Testing

All compression tests, including those at atmospheric pressure, were conducted in the pressure vessel. To prevent any build-up of pressure for atmospheric tests, the piston packing was removed. Shims were used to center the 0.480-inch-wide specimen in the 0.500-inch-wide slots of the fixtures. These shims were left in place while the set screws were tightened to a torque of 50 inches per pound. Tests using the Ultem specimens showed that this torque

was within a range where maximum values of compression strength were achieved. The torque was applied to the set screws while the fixtures and mounted specimen were inside a precision subpress having the same bore diameter as the pressure vessel. This step insured proper alignment of the specimen and fixtures. All tests were conducted at a stroke rate of 0.05 inches per minute measured remotely at the actuator of the test machine.

In order to establish confidence in the results obtained at high pressure, compression tests were also conducted at atmospheric pressure and 40 ksi on polycarbonate (PC) and 6061 aluminum. Polycarbonate has been shown to exhibit a large change in mechanical response with pressure,[4] while aluminum, like many metals, is relatively insensitive to the pressures of interest here.[5,6] For these tests, direct compression of specimens having a 2:1 aspect ratio of length to width were conducted in the pressure vessel.

Results and Discussion

The results of compression testing various IM7/8551-7 laminates at atmospheric pressure are summarized in Table 2. Also listed in the table is the calculated stress in the primary, load-bearing 0° ply at failure. This stress is calculated using classical lamination theory, which assumes linear elastic behavior for all plies. It is used to evaluate the "true" compression strength of the material as well as determine if failure occurred by a mechanism other than pure longitudinal compression. For comparison, manufacturer's data for this composite system give a unidirectional (longitudinal) compression strength in the range 243–252 ksi.[7] Strength values similar to this range are seen for the 0° plies of all the laminates except the one containing ±30 plies. Chris Hoppel of ARL has analyzed this laminate and believes it fails prematurely due to excessive transverse tensile stresses in the 0° plies. The Poisson's ratio for this laminate is approximately 1.1 and calculated transverse tensile stresses are close to ultimate values when this laminate fails at 207-ksi compression. The most telling observation is the mode of failure. The failure surface of most of the laminates is a shear-type fracture oriented at about 70° with respect to the load direction (the 0° direction). These fractures were confined to the gage section with many appearing to have initiated at one tab end. In contrast, ±30 laminates failed cleanly along one of the 30° lines, with the fibers in the opposite 30° ply and the 0° ply completely severed. At this angle, the failure propagated well into the tab area but appeared to initiate in the gage section near the tab. High-pressure tests with this laminate will be completed in the near future, and the potential for suppressing this mode of failure will be examined.

Table 2. Compression strengths of IM7/8551-7 laminates at atmospheric pressure.

Laminate	Compression Strength (ksi)	0° Ply Stress at Failure (ksi)
0_{16}	231	231
0_{16} (no tape)[(1)]	211	211
90_{16}	32.6	NA
$[45/90/-45/0]_{2S}$	96.1	252
$[90/0]_{4S}$	146.3	278
$[60/0/-60/0]_{2S}$	133.7	250
$[45/0/-45/0]_{2S}$	149.8	262
$[30/0/-30/0]_{2S}$	145.5	207

(1) Bonded to tabs without Kapton tape.

One of the biggest challenges in testing composites is the measurement of unidirectional compression strengths. In fact, the subject is updated yearly by D. F. Adams of the University of Wyoming.[8] The encouraging results by the group at Imperial College convinced us to adapt their technique to our high-pressure tests.[3] Using a modified version of this technique, the unidirectional strengths were found to be within 10% of the effective 0° ply strengths of the laminates. All failures occurred in the gage section near one tab. Testing of this specimen at high superimposed pressure resulted in failures occurring inside the tab region at the end of the Kapton tape, where the adhesive bondline started. There was some evidence that the pressurized kerosene was interacting with the tape adhesive. These results were interpreted as a change in failure mode and an attempt to circumvent this problem was made by simply preparing the specimen without the tape. The ambient pressure test results for this specimen are also given in Table 2 and show, as also shown by Matthews,[3] that without tape the strength is lower by about 10%. Nevertheless, since no change in failure mode was found at high pressures, these lower strength specimens were used to determine the effect of pressure on compression strength.

The high-pressure tests rely on pressure control in the supply line to the intensifier. The supply line pressure is well-controlled by the servohydraulic feed system to a maximum of 6,250 psi. This pressure is amplified in a 16:1 200-ksi intensifier, and some fidelity in pressure control is lost in this process. The friction in the intensifier seals must be overcome before its piston can move and communicate with the supply line. Until this friction is overcome, there is a pressure build-up as the piston enters the vessel and compresses the kerosene. Once the intensifier moves, the pressure is controlled usually to within 500 psi. For testing at a fixed pressure, the supply line is set to generate an initially lower pressure and the remaining build-up occurs during the kerosene compression. An example of this switch from stagnant behavior to active pressure control at 75 psi is shown in Figure 3. In this particular case, the pressure was originally set at 60 ksi and an additional 15 ksi was generated before pressure control was initiated. Once started, the control of vessel pressure is adequate. Also shown in this figure is some response at the pressure gage due to the spike generated when

the composite specimen failed. Because the system lacks adequate dynamic response, the actual pressure generated could not be measured.

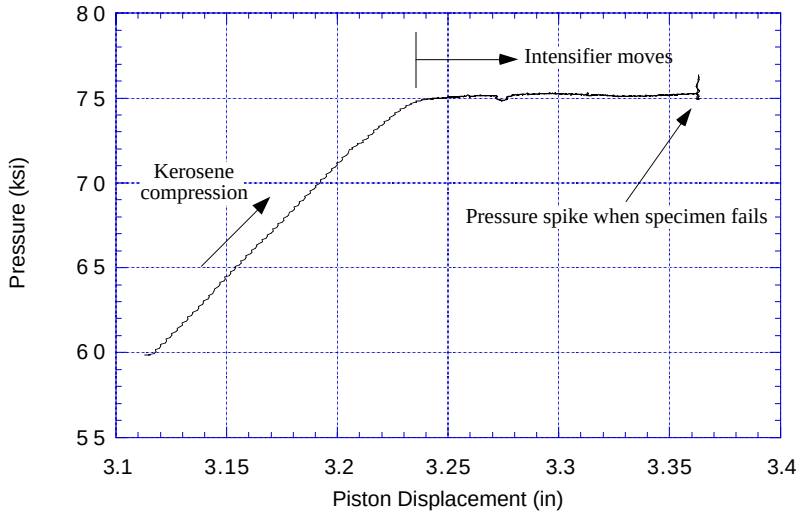

Figure 3. Pressure control in vessel after friction in intensifier is overcome.

The test results for the PC at atmospheric and 40-ksi pressures are shown in Figure 4. Also shown are data from an earlier study by Spitzig and Richmond[4] of hydrostatic pressure effects on tensile and compressive behavior of PC. Both the change in shape and magnitudes of the engineering stress-strain curves are similar. The data have been corrected for the change in dimensions of the specimens at elevated pressure due to the compressibility.[9] Although our tests were performed on a weaker grade of PC, the relative change in the compression response at 40 ksi is virtually identical to the previous result.

Results for compression testing of aluminum at 40 ksi are given in Figure 5. As expected, there is only a slight change in response toward higher yield and flow stresses. Metals are normally considered pressure-insensitive in this range of hydrostatic pressure and simple Mises-type yield criteria are usually adequate to define the failure under multiaxial stresses.

The most complete set of data to date for the composite specimens is for the unidirectional laminates that were prepared without the Kapton tape insert. The results of testing at atmospheric, 25-, 50-, and 75-ksi pressures are plotted in Figure 6. These data have been corrected for the reduction in specimen cross-sectional area due to pressure. Assuming linear behavior, this correction is calculated to be a 0.082% loss in area per ksi of hydrostatic pressure. At 75 ksi, this correction increases the strength by 6.6%, which is not trivial considering the magnitude of the strength changes measured.

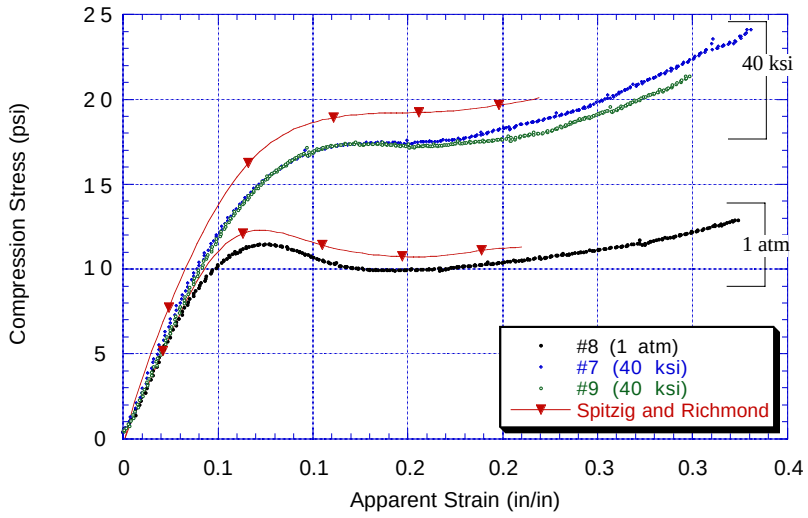

Figure 4. Effect of 40-ksi hydrostatic pressure on the compression response of polycarbonate.

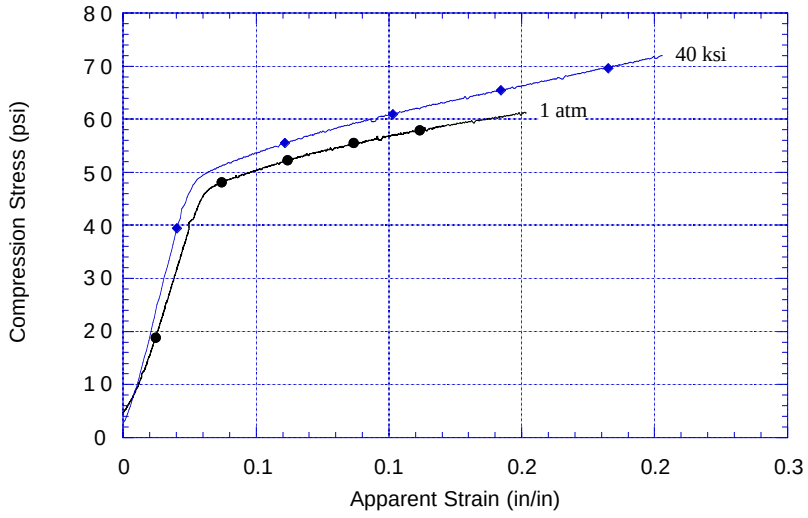

Figure 5. Effect of 40-ksi hydrostatic pressure on the compression response of 6061 aluminum.

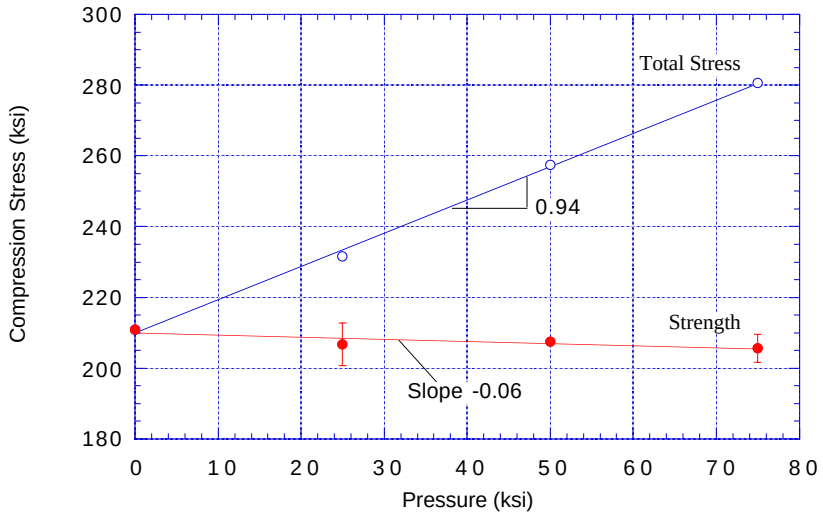

Figure 6. Effect of hydrostatic pressure on the longitudinal compression strength of unidirectional IM7/8551-7.

The two lines shown in Figure 6 represent the total stress in the loading direction and the strength, which is defined as the total stress at failure minus the pressure. There can be some confusion as to what constitutes a pressure-sensitive material if only the results for total stress are considered. The change in total stress, σ_{11}, at failure is commonly expressed as a linear function of superimposed hydrostatic pressure, P:

$$\sigma_{11} = \sigma_o^u + aP \tag{1}$$

where σ_o^u is the strength at ambient pressure. In terms of the stress difference at failure, which we define as the strength, σ^u:

$$\sigma^u \equiv \sigma_{11} - P = \sigma_o^u + (a-1)P \tag{2}$$

For a pressure-insensitive or Mises-type material, the constant a in (1) and (2) is unity and there is no change in *strength* with pressure. The preliminary results summarized in Figure 6 indicate that pressure has little effect on compression strength. However, these results must be viewed with caution since the test method does not yield the higher material strength calculated from multidirectional laminates. Although specimens failed in the same manner at all pressures, it is possible that a true compression strength is not being measured.

The reason for plotting the total stress on the specimen is for comparison with other experimental and theoretical results. Several studies have reported strength changes in unidirectional fiber composites due to pressure.[10–13] Most of these studies were performed on simple, uniformly shaped specimens, which invariably fail due to stress concentrations at the ends. Therefore, the results of these studies are difficult to interpret. The one study where

gage failures and reasonable ambient pressure compression strengths for a 60-vol.-%, carbon fiber composite were reported is that by Parry and Wronski.[11] Their results were obtained using an external load cell that was corrected for friction effects. They showed that the total stress at failure increased first with a slope of 0.6 to about 20 ksi and thereafter at a slope of 3.2 up to the maximum test pressure of 43.5 ksi. They attributed the slope change to a transition from longitudinal shear failure to kinking compression failure at 20 ksi. When considered in terms of strength, as we have defined here, their results show that strength first decreases at a rate of -0.4 (i.e., 0.6-1) and then increases at a rate of 2.2 with hydrostatic pressure. Furthermore, if these results are corrected for specimen compressibility (the authors make no mention of doing so), then the slopes for strength below and above 20 ksi change to approximately –0.2 and 2.4, respectively. Seen in this form, the lower pressure results are not very different from what we have measured here.

While the decrease in strength seems to contradict the results of other studies, it does agree with some theoretical results from interactive failure models.[14-16] In these models, the strength difference in compression and tension, normally observed for fiber-direction loading, is a result of a dependence of strength on hydrostatic pressure. When the magnitude of the strength in compression is less than tension, which is typical for carbon fiber composites, the models predict a decrease in compression strength under superimposed hydrostatic pressure. Alternatively, under these conditions the predicted slope between total compression stress and pressure is less than one. Our early results confirm this trend, but further refinement of the unidirectional test is needed before the quantitative relationship between strength and pressure can be measured.

For failure in the transverse direction, compression strengths exceed those in tension and the failure models predict an enhancement in compression strength with pressure. We have seen this effect, as shown in Figure 7. The relatively large change in strength with pressure is due to the same factors controlling the failure of isotropic polymeric materials, namely, a significant strength difference in tension and compression and relatively low strength magnitudes. We are continuing these tests to determine the quantitative relationship between strength and pressure for matrix-dominated failure modes.

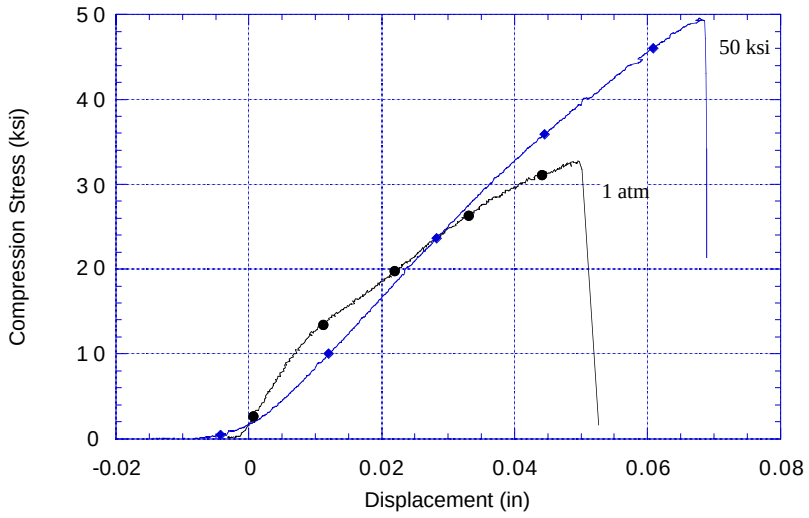

Figure 7. Effect of hydrostatic pressure on the transverse compression properties of unidirectional IM7/8551-7.

Conclusions

We have begun to measure the effects of superimposed hydrostatic pressure on the fiber-direction strengths of carbon-fiber composites. Preliminary results with unidirectional materials are qualitatively similar to recent theoretical predictions. However, further development of the specimen is needed before reliable strengths can be achieved. We are investigating methods that circumvent failure due to high stresses at the tabs. An observed increase in transverse compression with pressure also agrees with theoretical predictions. The multidirectional laminates appear to yield consistent compression strengths at atmospheric pressures and are currently being tested at high pressures.

Acknowledgments

We are grateful to the contributions made by others to this work—to Will Andrade for his help in designing and machining improvements to the fixture and the load cell, to Pat Harwood for assembling the pressure test system, and to Rich Ring for applying the strain gages to the load cell. The donation of AS4/Ultem panels and prepreg by Joe Morris is greatly appreciated. We also appreciate the helpful advice of Dr. Rosanna Falabella of Hexcel Corp. and Professor Frank L. Matthews of Imperial College on testing unidirectional composites and the advice from Brian Bonner, Carl Boro, and Bill Ralph on the art and science of high-pressure testing. The discussions with Chris Hoppel of ARL have provided important guidance to this project.

References

1. C. P. R. Hoppel, T. A. Bogetti, and J. W. Gillespie, Jr., *Effects of Hydrostatic Pressure on the Mechanical Behavior of Composite Materials*, Army Research Laboratory, ARL-TR-727 (April 1995).

2. P. W. Bridgman, "The Effect of Pressure on the Viscosity of Forty-Three Pure Liquids," *Proc. Am. Acad. Arts Sci.* **61**, 57–99 (1926).

3. J. G. Haberle and F. L. Matthews, "An Improved Technique for Compression Testing of Unidirectional Fibre-Reinforced Plastics; Development and Results," *Composites,* **25**(5), 358–371 (1994).

4. W. A. Spitzig and O. Richmond, "Effect of Hydrostatic Pressure on the Deformation Behavior of Polyethylene and Polycarbonate in Tension and Compression," *Polym. Eng. Sci.* **19**(16), 1129–1139 (1979).

5. P. W. Bridgman, "Effect of Hydrostatic Pressure on Plasticity and Strength," *Research* (London) **2,** 550–555 (1949).

6. H. L. D. Pugh, "Mechanical Properties and Deformation Characteristics of Metals and Alloys Under Pressure," *Irreversible Effects of High Pressure and Temperature on Materials*, American Society for Testing and Materials, STP No. 374 (1965).

7. Magnamite® 8551-7 Tough Resin, Graphite Prepreg Tape and Fabric Summary, Hercules Aerospace Products Group, Bacchus Works, Magna, UT, (November 1985), and Product Data Sheet.

8. J. S. Welsh and D. F. Adams, "Current Status of Compression Test Methods for Composite Materials," *SAMPE J.* **33**(1), 35–43 (1997).

9. R. W. Warfield, "Compressibility of Linear Polymers," *J. Appl. Chem.* **17,** 263–268 (1967).

10. C. W. Weaver and J. G. Williams, "Deformation of a Carbon-Epoxy Composite under Hydrostatic Pressure," *J. Mater. Sci.,* **10,** 1323–1333 (1975).

11. T. V. Parry and A. S. Wronski, "Kinking and Compressive Failure in Uniaxially Aligned Carbon Fibre Composite Tested under Superposed Hydrostatic Pressure," *J. Mater. Sci.,* **17,** 893–900 (1982).

12. A. S. Wronski and T. V. Parry, "Compressive Failure and Kinking in Uniaxially Aligned Glass-Resin Composite under Superposed Hydrostatic Pressure," *J. Mater. Sci*., **17,** 3656–3662 (1982).

13. K. Y. Rhee and K. D. Pae, "Effects of Hydrostatic Pressure on the Compressive Properties of Laminated, 0˚ Unidirectional, Graphite Fiber/Epoxy Matrix Thick-Composite," *J. Comp. Mater*., **29**(10), 1295–1307 (1995).

14. W. W. Feng, "A Failure Criterion for Composite Materials," *J. Comp. Mater*., **25**(1), 88–100 (1991).

15. R. M. Christensen, “Stress Based Yield/Failure Criteria for Fiber Composites,*”* *Int. J. Solids Struct*. **34**(5), 529–543 (1997).

16. R. M. Christensen, “Tensor Transformations and Failure Criteria for the Analysis of Fiber Composite Materials,” *J. Comp. Mater*., **24**(8), 796–800 (1990).